CORROSION BEHAVIOUR OF HIGHLY CREEP RESISTANT MAGNESIUM-RARE-EARTH-BASED ALLOYS

VOLKMAR NEUBERT[1,3], IVANA STULÍKOVÁ[1,2], BOHUMIL SMOLA[1,2]*,
ASHRAF BAKKAR[3], BARRY LESLIE MORDIKE[1,4]

Highly creep resistant magnesium alloys containing Sc, rare earths (Gd, Ce, Nd, Y) and manganese exhibit a considerably higher corrosion resistance than high purity magnesium. This is attributed to the beneficial effect of rare earth elements on the stability of the protective surface layer, presumably magnesium hydride MgH_2, deposited on the surface as a corrosion product. Ternary MgSc15Mn1 and quaternary MgSc6Ce4Mn1 behave differently. This is due to the high Sc content and its distribution (segregation and undissolved particles). The presence of intermetallic phases (Mg-rare earth) has no detrimental effect on the corrosion resistance, but the $Mg_{12}Ce$ phase can contribute to the high corrosion rate in alloys with a high Sc content.

K e y   w o r d s: Mg alloys, rare earths, creep resistance, corrosion resistance

KOROZNÍ CHOVÁNÍ SLITIN NA BÁZI HOŘČÍK-VZÁCNÁ ZEMINA S VYSOKOU ODOLNOSTÍ PROTI TEČENÍ

Hořčíkové slitiny s vysokou odolností proti tečení, které obsahují skandium, vzácné zeminy (Gd, Ce, Nd, Y) a mangan, jsou výrazně odolnější proti korozi než velmi čistý hořčík. Tento efekt je připisován pozitivnímu vlivu prvků vzácných zemin na stabilitu ochranné povrchové vrstvy, pravděpodobně tvořené hydridem hořčíku MgH_2, která se v důsledku koroze na povrchu vytváří. Ternární slitina MgSc15Mn1 a kvaternární slitina MgSc6Ce4Mn1 se chovají odlišně díky vysokému obsahu Sc a jeho rozdělení (segregace a nerozpuštěné částice). Přítomnost intermetalických fází (Mg-vzácná zemina) nemá škodlivý vliv na korozní odolnost, ovšem ve slitinách s vysokým obsahem Sc může fáze $Mg_{12}Ce$ přispívat k vysoké korozní rychlosti.

[1] Zentrum für Funktionswerkstoffe GmbH, Sachsenweg 8, Clausthal-Zellerfeld, Germany
[2] Faculty of Mathematics and Physics, Charles University, Ke Karlovu 5, Prague 2, Czech Republic
[3] Institut für Materialprüfung und Werkstofftechnik, DN GmbH, Freibergerstr. 1, Clausthal-Zellerfeld, Germany
[4] Institut für Werkstoffkunde und Werkstofftechnik, TU Clausthal, Agricolastr. 6, Clausthal-Zellerfeld, Germany
* corresponding author, e-mail: `bohumil.smola@mff.cuni.cz`

1. Introduction

Recently a worldwide interest in the increasing of magnesium alloys application as construction materials evokes an increased research into a variety of properties also on national levels (e.g. [1, 2]). Magnesium alloys for applications at higher temperatures should exhibit not only high strength, creep resistance and stability, but also good corrosion resistance. Rare earth elements (RE), which are frequent additions in such alloys, are known to improve poor corrosion resistance of magnesium [3, 4]. High corrosion resistance of the AZ91D alloy, which is comparable to carbon steel in salt spray environment, can be explained by three attributes, namely: 1. an electrochemically passive intermetallic network, 2. intermetallics trapping cathodic impurities and 3. enrichment of oxide layer by aluminium. These attributes would appear not to account for the effect of the RE elements. On the contrary, the formation of magnesium hydride MgH_2 layer, which may work as barrier against further dissolution of Mg, was found to be enhanced by the RE addition. This conclusion was drawn from results of corrosion behaviour studies of the commercial WE54 alloy as well as other Mg alloys containing Gd, Dy, Nd, Y, or combinations thereof [3, 4]. Another element, manganese, is also recognised as a useful addition to Mg, as it binds the corrosion-enhancing iron into Fe-Mn compounds and thus improves corrosion resistance of Mg alloys [5].

Recently, experimental, highly creep resistant Mg alloys containing scandium, RE including Y and manganese were developed for applications at temperatures up to 350 °C [6–11]. The basic corrosion characteristics of these alloys are presented and discussed here from the viewpoint of the precipitation structure observed.

2. Experimental details

Experimental Mg alloys were squeeze cast under a protective gas atmosphere (Ar + 1 % SF_6). The phase composition and the structure and distribution of the precipitates in cast alloys were determined by transmission electron microscopy and electron diffraction with the additional support of energy dispersive X-ray microanalysis (JEOL JEM 2000FX equipped for microanalysis using a LINK AN10000).

The corrosion behaviour was studied by using electrochemical and hydrogen evolution tests. Samples were cut into $12 \times 12 \times 6$ mm^3 blocks. Those for potentiodynamic polarisation tests had copper wires welded onto one side and were mounted in Struers Epofix cold-setting resin. They were suspended in the electrolyte, exposing the 12×12 mm^2 test surface. In both types of test, a fresh surface was obtained by grinding up to 1200 grit SiC paper using ethanol, as a lubricant and cooler. Finally, the specimens were ultrasonically cleaned with several rinses of ethanol and immediately placed into the electrolyte. All experiments were carried out at 25 ± 1 °C.

Potentiodynamic polarisation experiments were carried out using a Wenking

LB 94L (Auto Range) Laboratory Potentiostat, controlled by a PC computer. The specimen was immersed in 100 ppm NaCl solution for 15 minutes prior to polarisation, by which time a stable potential, open circuit potential (OCP) was obtained. A saturated calomel electrode was used as a reference. Polarisation was obtained by scanning from 500 mV more negative than the OCP at a rate of 20 mV/min. The pH was adjusted to 12 by adding NaOH.

The hydrogen evolution measurements consisted of putting the Mg specimen onto a glass seat in a beaker glass containing 1200 ml of 3 % NaCl borax-buffered solution with a pH = 9.3. A burette with a funnel end was then placed over the specimen, to collect all the hydrogen generated on the specimen surface.

3. Results and discussion

3.1 Composition and structure of experimental alloys

The composition of the alloys studied, determined by atomic absorption, is listed in Table 1 together with the measured and calculated densities. It is clear that squeeze casting ensures very low porosity in the alloys. The average grain size of the as-squeeze-cast alloys was in the range of 45 to 100 μm – see Table 2 [9, 11, 12]. Binary MgSc10 and ternary MgSc15Mn1 alloys exhibited pronounced segregation of Sc and part of Sc remains undissolved.

Table 1. Composition and density of squeeze cast alloys

Alloy	Gd [wt.%]	Y [wt.%]	Ce [wt.%]	Nd [wt.%]	Sc [wt.%]	Mn [wt.%]	Density [kg·m^{-3}]	
							Meas.	Calc.
MgSc10	–	–	–	–	10.14	–	1821	1817
MgSc15Mn1	–	–	–	–	15.2	1.4	1876	1880
MgSc6Ce4Mn1	–	–	4.2	–	6.3	1.5	1841	1869
MgCe3Sc1Mn1	–	–	2.84	–	0.92	1.13	1790	1800
MgGd5Sc1Mn1	4.64	–	–	–	0.26	1.53	1835	1830
MgGd10Sc1Mn1	9.63	–	–	–	0.91	1.30	1892	1909
MgY4Sc1Mn1	–	3.88	–	–	0.73	1.11	1794	1805
MgY4Nd2Sc1Mn1	–	3.71	–	2.12	1.28	1.18	1846	1837

Table 2. Average grain size of squeeze cast alloys

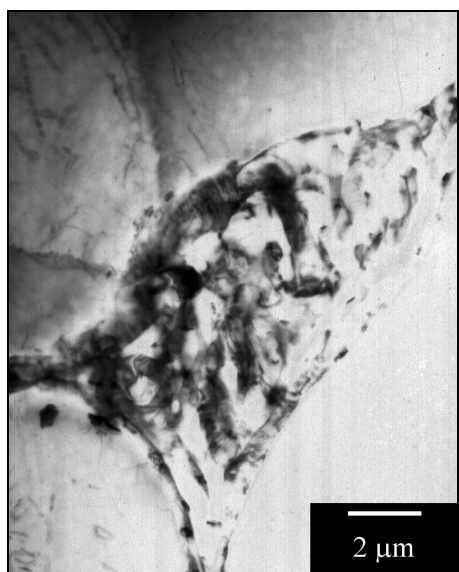| Alloy	Grain size [μm]	Alloy	Grain size [μm]
MgSc10	60	MgGd5Sc1Mn1	100
MgSc15Mn1	100	MgGd10Sc1Mn1	100
MgSc6Ce4Mn1	45	MgY4Sc1Mn1	70
MgCe3Sc1Mn1	70	MgY4Nd2Sc1Mn1	80

Fig. 1. Grain boundary eutectic in the as-
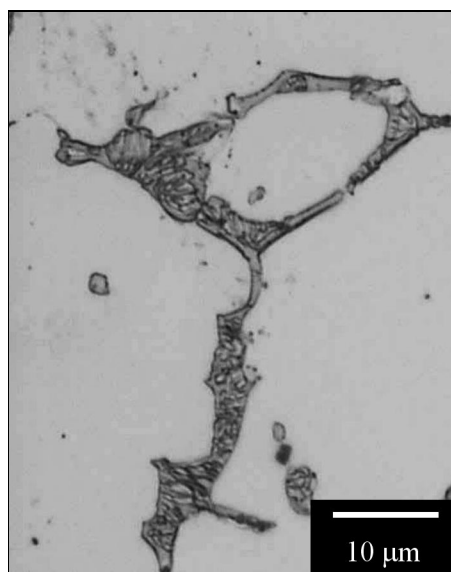cast MgSc6Ce4Mn1 alloy.

Fig. 2. Grain boundary eutectic in the as-
cast MgY4Nd2Sc1Mn1 alloy.

In both the alloys containing Ce, a grain boundary (GB) eutectic, consisting of the α-Mg matrix (solid solution of Ce, Sc and Mn in Mg with cph structure) and the $Mg_{12}Ce$ stable phase (tetragonal bc structure, $a = 1.033$ nm, $c = 0.596$ nm), forms due to the low Ce solubility in Mg (Fig. 1). Also in the MgY4Nd2Sc1Mn1 alloy the GB eutectic, consisting of the α-Mg matrix and the equilibrium Mg-Y-Nd phase (the β phase known from WE alloys, is isomorphous with the Mg_5Gd, fcc structure, $a = 2.223$ nm) was observed (Fig. 2).

The grain boundaries in all alloys are irregularly (more or less densely) decorated by coarse particles containing Sc and Mn (size ~ 1 μm; ~ 30–100 nm in MgY4Sc1Nd1), presumably of the Mn_2Sc phase (hexagonal $P6_3$/mmc, $a = 0.5033$ nm, $c = 0.8278$ nm). These particles alternate with those of the equilibrium phases $Mg_{24}Y_5$ (bcc Mn type structure, $a = 1.128$ nm) and the Mg_5Gd (fcc structure, $a = 2.234$ nm) in the Y and Gd containing alloys, respectively (Fig. 3). Square shaped plates (each side ~ 1 μm) of either fcc modification of pure Gd (Y) ($a = 0.54$ nm) or Gd (Y) oxide with the same structure and lattice parameter were observed in alloys with corresponding RE both in the grain boundaries and grain interior.

Although squeeze casting is a process with relatively rapid cooling during solidification, a certain volume fraction of transient and stable phases precipitates within the grains. The Mn_2Sc phase plates form rosette-like structures (diameter
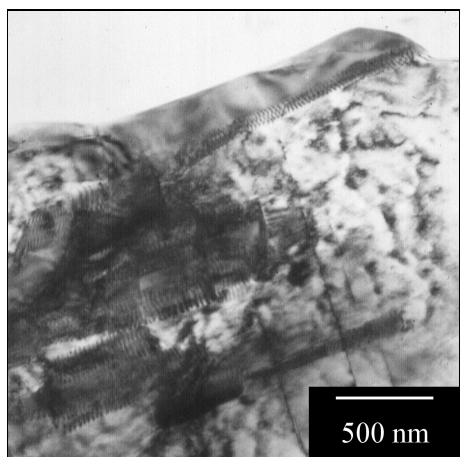
Fig. 3. $Mg_{24}Y_5$ particle in the grain bound-
ary of the as-cast MgY4Sc1Mn1 alloy.

Fig. 4. "Ribbon" like modification of the
$Mg_{12}Ce$ stable phase in the as-cast MgCe-
3Sc1Mn1 alloy in the [0001] direction of the
α-Mg matrix.

~ 2.5 μm), irregularly distributed within the grains of the ternary MgSc15Mn1 alloy together with smaller particles of the same phase (size ~ 100 nm) [7].

The matrix grains of the quaternary MgSc6Ce4Mn1 alloy contain a dense arrangement of dislocations decorated by Ce rich plates parallel to the $\{1\bar{1}00\}_{Mg}$ planes (diameter ~ 100–200 nm, thickness ~ 15–20 nm) [7]. These plates are, most probably, the β' transient phase of the Mg-Nd decomposition sequence [13] (fcc structure, $a = 0.743$ nm). On the other hand, various forms of the stable $Mg_{12}Ce$ phase were observed within the grains of the as-cast MgCe3Sc1Mn1 alloy, namely rods parallel to $[0001]_{Mg}$ direction (~ 150 nm long, ~ 50 nm in the cross section), plates parallel to $\{11\bar{2}0\}_{Mg}$ planes (~ 200 nm diameter, ~ 10 nm thickness), and ribbon-like precipitates (Fig. 4) formed by stacking of plates parallel to $\{11\bar{2}0\}_{Mg}$ planes in $[0001]_{Mg}$ direction [11].

Fine discs of the Mn_2Sc phase (diameter ~ 10–15 nm, thickness ~ 3 nm) in the basal planes of α-Mg matrix are arranged into "ribbons" parallel to the basal planes in the MgGd5Sc1Mn1 alloy (Fig. 5) [11]. These discs were observed neither in the as-cast MgGd10Sc1Mn1 nor in the MgY4Sc1Mn1 and MgY4Nd2Sc1Mn1 alloys [11, 14].

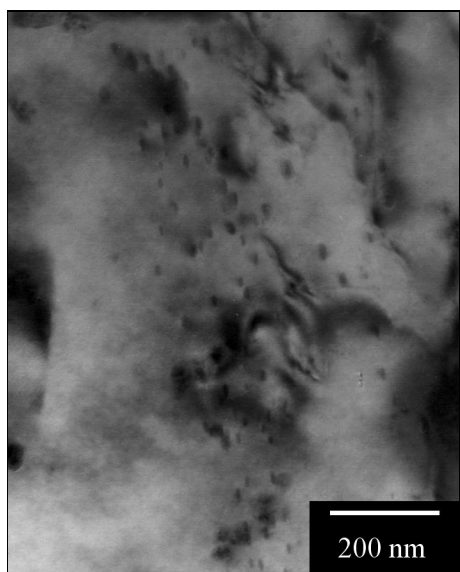Thermodynamic calculations of equilibrium phase diagrams of ternary Mg-Sc-

Fig. 5. Mn$_2$Sc basal discs in the as-cast MgGd5Sc1Mn1 alloy arranged in "ribbons" parallel to the (0001) planes of the α-Mg matrix.
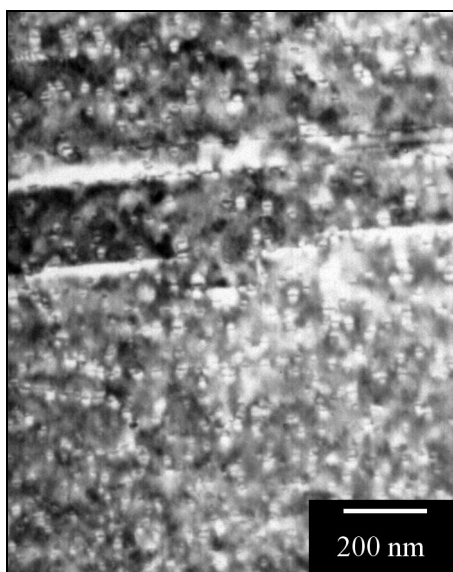
Fig. 6. Mn$_2$Sc basal discs in the MgY4Sc1-Mn1 alloy crept at 350 °C/30 MPa.

-Mn [15] and quaternary Mg-Gd(Y)-Sc-Mn [16] alloys show the practical impossibility of homogenisation or solution heat treatments (T4 temper). The Mn$_2$Sc equilibrium phase precipitates during solidification and a subsequent heat treatment up to solidus or liquidus temperature. It precipitates in the form of very small particles in the MgSc15Mn1 alloy (size $\sim$ 4.5 nm) and as fine discs parallel to the basal planes of α-Mg matrix in all other Sc and Mn containing alloys (diameter 10–25 nm, thickness 3–5 nm) during heat treatment leading to peak age hardening (T5 temper) [8].

The creep behaviour is strongly influenced by the presence of Mn$_2$Sc fine discs embedded in the matrix parallel to basal planes. The discs, which develop during creep deformation, do not grow, even at 350 °C (Fig. 6). Minimum creep rates derived from creep tests at 350 °C and 30 MPa are compared in Table 3. The minimum creep rate of the MgSc10 alloy in the T4 treated state is of three or four orders of magnitude higher than those of alloys containing the Mn$_2$Sc phase. Slight differences in the minimum creep rate of about one order of magnitude among the alloys containing the Mn$_2$Sc phase are caused by differences in the volume fraction of Mn$_2$Sc and the presence of other precipitates, as for example the Mg$_5$Gd, β phase in the MgY4Nd2Sc1Mn1 alloy or the Mg$_{24}$Y$_5$ stable phase. All these types

Table 3. Minimum creep rates at $T = 350\,°C$, $\sigma = 30$ MPa. MgSc10 was solution-treated (T4) before the creep test. All other alloys were in the as-cast state

Alloy	$\dot{\varepsilon}_{\min}$ [s^{-1}]
MgSc10	1.84×10^{-4}
MgSc15Mn1	3.8×10^{-8}
MgSc6Ce4Mn1	4.6×10^{-8}
MgCe3Sc1Mn1	1.5×10^{-8}
MgGd5Sc1Mn1	2.5×10^{-8}
MgGd10Sc1Mn1	2.7×10^{-8}
MgY4Sc1Mn1	6.6×10^{-8}
MgY4Nd2Sc1Mn1	1.8×10^{-7}

of particles, in the form of plates, are oriented perpendicular to basal planes and do not contribute as effectively to the creep resistance. They develop either in the as-cast state or the T5 state, where corresponding transient phases had formed. Due to the differences in volume fraction and the size of stable precipitates, the T5 treated alloys exhibited slightly lower minimum creep rates at $350\,°C$ than the alloys in the as-cast state at the same temperature [8, 17].

3.2 Corrosion characteristics of as-cast alloys

The corrosion characteristics of alloys investigated, which were obtained by potentiodynamic polarisation, are shown in Table 4 and Fig. 7. A notable and clear feature is the large difference between the free corrosion potential, namely OCP, and the corrosion potential (E_{corr}), obtained from polarisation curves by extrapolation of Tafel lines. It is clear that polarisation in the cathodic region shifts E_{corr} in the more noble direction with values ranging from 284 to 615 mV.

This result implies that, during the cathodic polarisation, some hydrogen ions are discharged and partially diffuse into the Mg-RE cathode, forming a protective

Table 4. Corrosion characteristics of some Mg-RE alloys obtained by polarisation in 100 ppm NaCl solution, pH = 12

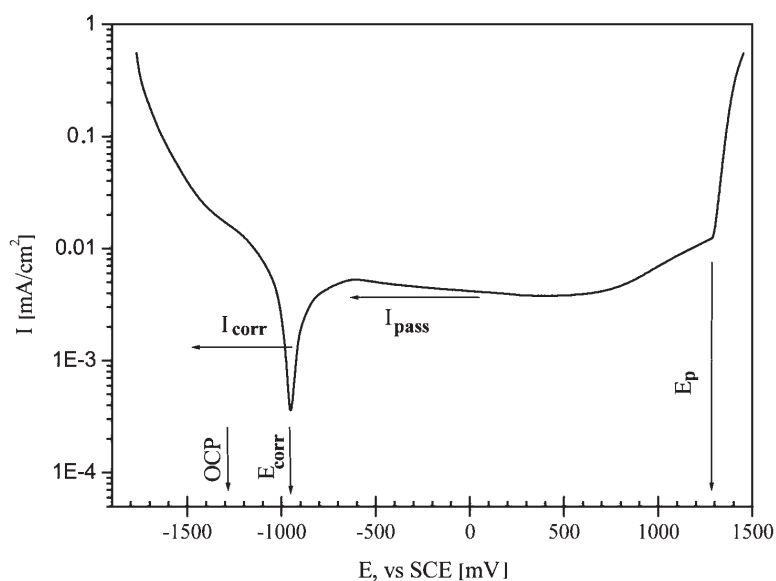| Alloy	OCP [mV]	E_{corr} [mV]	I_{corr} [μA/cm^2]	E_p [mV]	I_{pass} [μA/cm^2]
MgSc10	-1390	-843	1.559	$+620$	2.83
MgSc15Mn1	-1366	-1082	0.724	-150	3.97
MgSc6Ce4Mn1	-1250	-913	1.449	-755	$-$
MgGd5Sc1Mn1	-1330	-788	1.157	$+1215$	1.73
MgGd10Sc1Mn1	-1350	-735	1.22	$+1259$	1.83
MgY4Sc1Mn1	-1279	-947	1.273	$+1320$	3.71

Fig. 7. The potentiodynamic polarisation diagram for the MgY4Sc1Mn1 alloy in a 100
    ppm NaCl solution; pH $= 12$ (to show the parameters monitored in Table 4).

hydride. It has been reported, that a corrosion barrier of magnesium hydride is
spontaneously formed on the RE rich Mg-based alloys [3, 4]. Furthermore, the for-
mation of the magnesium dihydride, MgH_2 layer, was demonstrated [4]. A markedly
improved corrosion and oxidation resistance after adding RE – (1 to 2 wt.%) – to
the AM50-Mg alloy, has been reported [18]. The beneficial effect of RE was at-
tributed to the eventual stabilisation of the surface layer formed.

   Referring to Table 4, the pitting potential (E_p) is considered to be the only
corrosion parameter capable of enabling a comparison between the alloys studied.
It was also shown, that the pitting potential is the most suitable parameter for
comparing corrosion of various Mg alloys in alkaline electrolyte [19]. It can be
seen that the presence of Sc in high amounts has a deleterious effect, reducing the
pitting potential to more negative values. In other words, high Sc contents appear
to reduce the stability of the MgH_2 formed. Contrary to the effect of Sc, Gd, even
at high concentrations, maintains the pitting potential at more noble values.

   For a better comparison of the corrosion behaviour of the alloys studied, the
free hydrogen evolution was measured and monitored (Fig. 8). With respect to
the hydrogen evolution after 50 and 100 h, it is clear that the corrosion rates of
all Mg-RE alloys studied are significantly lower than that of high purity magne-
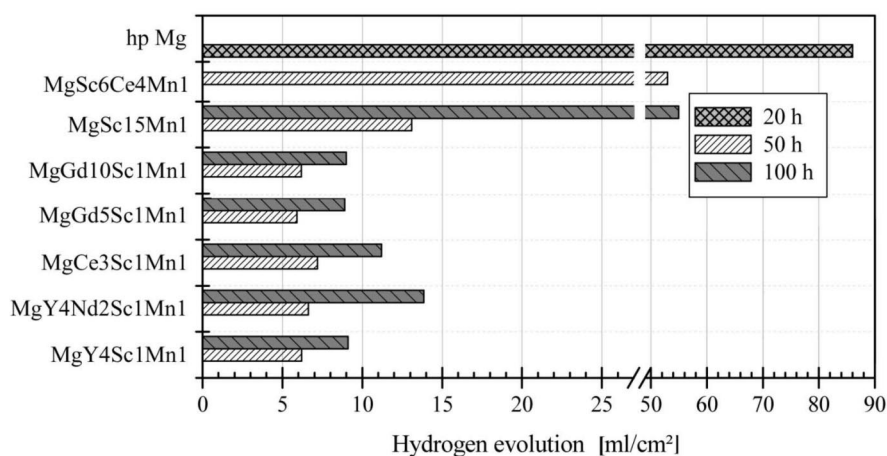sium (hp) Mg. Also, it can be seen that the alloys, which have the low pitting

Fig. 8. Hydrogen evolution rates of high purity Mg and Mg-RE alloys in a 3 % NaCl solution; pH = 9.3.

potential E_p, monitored in Table 4, exhibit high corrosion rates. Additionally, the corrosion rate enhancing effect by high concentrations of Sc is confirmed. On the other hand, the alloys containing 5 wt.% and 10 wt.% Gd have the lowest rate of H_2-evolution, recording very close values. Thus, increasing the amount of Gd to contents over 5 wt.% introduces neither deleterious nor beneficial effects on the corrosion resistance.

For each alloy, by dividing the recorded value of H_2-evolution after 50 h by that after 100 h, the result will be a proper fraction. If this fraction is $1/2$, this means that the corrosion rate of alloy is constant with immersion time. It should be pointed out that the alloys, which have low H_2-evolution values, have a fraction $> 1/2$, indicating a decrease in corrosion rate with time. This decrease in corrosion rate is attributed to the protective nature of the corrosion product films deposited on those alloys.

The microstructural evidence presented above shows that the corrosion behaviour of the Mg-RE alloys is strongly influenced by the precipitation of intermetallic compounds. The high corrosion rate, associated with high concentrations of scandium, can be clearly related to the segregation and its partly undissolved state for concentrations $\geq$ 10 wt.%. The presence of the Ce rich phase ($Mg_{12}Ce$) appears to have no detrimental effect on the corrosion resistance of Ce-containing alloys. However, the presence of this phase ($Mg_{12}Ce$) together with inherently dense dislocations is, most probably, the reason for the high corrosion rate of the MgSc6Ce4Mn1 alloy. Nevertheless, the great shift of E_{corr} in the more noble direction, observed in polarisation curves (Table 4), indicates that the protective film

(MgH_2) is formed on all Mg-RE alloys in spite of the presence of intermetallic compounds.

Consequently, it can be stated that RE elements are very valuable in improving the corrosion resistance of Mg-based alloys by stabilisation of the MgH_2 film formed as an intermediate step in the corrosion process. The MgH_2, which acts as a barrier against further corrosion, is formed onto Mg-RE base alloys regardless the presence of intermetallic compounds. Thereafter, these intermetallic compounds affect the stability of the MgH_2 formed.

4. Conclusion

Highly creep resistant magnesium-rare earth alloys with low contents of Sc and Mn ($\sim$ 1 wt.%) are much more corrosion resistant than pure magnesium. The corrosion resistance depends strongly on the distribution of the rare earth elements, and thus on the microstructure. The corrosion resistance deteriorates with increasing Sc content due to the segregation of Sc, both within the grain and that of undissolved particles. Except for those with low cathodic activities, the intermetallic compounds formed also reduce the corrosion resistance.

Acknowledgements

REFERENCES

[1] HADZIMA, B.—PALČEK, P.—CHALUPOVÁ, M.—ČANADY, R.: Kovove Mater., *41,* 2003, p. 257.

[2] TROJANOVÁ, Z.—KÚDELA, S.—LUKÁČ, P.—DROZD, Z.—PTÁČEK, L.—MÁTHIS, K.: Kovove Mater., *41,* 2003, p. 203.

[3] NAKATSUGAWA, I.—KAMADO, S.—KOJIMA, Y.—NINOMIYA, R.—KUBOTA, K.: In: Proc. 3rd Int. Magnesium Conference. Ed.: Lorimer, G. W. Cambridge, The Institute of Materials 1997, p. 687.

[4] NAKATSUGAWA, I.—KAMADO, S.—KOJIMA, Y.—NINOMIYA, R.—KUBOTA, K.: Corrosion Rev., *16*, 1998, p. 139.

[5] UNSWORTH, W.: Int. J. of Materials and Product Technology, *4*, 1989, p. 359.

[6] MORDIKE, B. L.: J. Mater. Process. Technology, *117*, 2001, p. 391.

[7] SMOLA, B.—STULÍKOVÁ, I.—PELCOVÁ, J.—VON BUCH, F.—MORDIKE, B. L.: Phys. stat. sol. (a), *191*, 2002, p. 305.

[8] SMOLA, B.—STULÍKOVÁ, I.—VON BUCH, F.—MORDIKE, B. L.: Mater. Sci. Eng. A, *324*, 2002, p. 113.

[9] SMOLA, B.—STULÍKOVÁ, I.—MORDIKE, B. L.: Phys. stat. sol. (a), *190*, 2002, p. R5.

[10] STULÍKOVÁ, I.—SMOLA, B.—VON BUCH, F.—MORDIKE, B. L.: Mat.-wiss. u. Werkstofftech., *34*, 2003, p. 102.

[11] SMOLA, B.—STULÍKOVÁ, I.—PELCOVÁ, J.—VON BUCH, F.—MORDIKE, B.
     L.: Z. Metallkde., *94*, 2003, p. 553.
[12] VON BUCH, F.: Entwicklung hochkriechbeständiger Magnesiumlegierungen des
     Typs Mg-Sc(-X-Y), Mg-Gd und Mg-Tb. [PhD thesis]. TU Clausthal 1999.
[13] LORIMER, G. W.: In: Proc. London Conf. Magnesium Technology. Ed.: Baker, H.
     London, Inst. of Metals 1986, p. 47.
[14] STULÍKOVÁ, I.—SMOLA, B.—PELCOVÁ, J.—MORDIKE, B. L.: Magnesium.
     Ed.: Kainer, K. U. Weinheim, Wiley-Vch Verlag 2004, p. 116.
[15] VON BUCH, F.—LIETZAU, J.—MORDIKE, B. L.—PISCH, A.—SCHMID-FET-
     ZER, R.: Mater. Sci. Eng. A, *263*, 1999, p. 1.
[16] GRÖBNER, J.—SCHMID-FETZER, R.: J. Alloys Compounds, *320*, 2001, p. 296.
[17] SMOLA, B.—STULÍKOVÁ, I.—PELCOVÁ, J.—MORDIKE, B. L.: Magnesium.
     Ed.: Kainer, K. U. Weinheim, Wiley-Vch Verlag 2004, p. 43.
[18] ALVES, H.—KÖSTER, U.: Magnesium Alloys and Their Applications. Ed.: Kainer,
     K.U. Weinheim, Wiley-Vch Verlag 2000, p. 439.
[19] NEUBERT, V.—BAKKAR, A.: Magnesium. Ed.: Kainer, K. U. Weinheim, Wiley-
     -Vch Verlag 2004, p. 638.